Neutron Shielding Design of Infrared Imaging Video Bolometer for LHD Deuterium Experiment

Kiyofumi Mukai, Takeo Nishitani, Kunihiro Ogawa, and Byron J. Peterson

***Abstract*— InfraRed imaging Video Bolometer (IRVB) is a powerful diagnostic for the plasma radiation measurement. Study on plasma radiation phenomena, e.g., plasma detachment is one of the crucial issues to realize a fusion reactor. In order to apply the IRVB to such a study, a shielding is required to protect an IR camera from neutron irradiation. In the Large Helical Device (LHD) deuterium experiment has started in 2017. Then, the shielding was designed using MCNP6 code with the three-dimensional modelling of LHD. The guideline of the neutron flux for the design was determined by the operational experience in JT-60U tokamak and by the result of the irradiation in OKTAVIAN. The strong neutron flux due to the location close to the vacuum vessel and the influx through the lens hole were reduced sufficiently. The designed shielding was applied to the LHD deuterium experiments and the IRVB with the shielding could be operated successfully without any dead pixels in the neutron emission rate up to 3.3 × 10^{15} n·s^{-1}, which is the maximum rate in the first experimental campaign, and in the total neutron emission of 3.6 × 10^{18} n. These correspond to the neutron emission rate of 2.9 × 10^{7} n·s^{-1} and the total neutron emission of 3.2 × 10^{10} n at around the IR camera.**

***Index Terms*— Bolometers, Imaging, Infrared image sensors, MCNP, Neutron shielding**

I. Introduction

PLASMA radiation measurement is one of the important diagnostics for the plasma fusion research in studying plasma phenomena, e.g., detachment and radiation collapse. Plasma radiation mainly occurs outside the last closed flux surface where the axis symmetry cannot be assumed. Therefore, multi-dimensional diagnostics are required. InfraRed imaging Video Bolometer (IRVB) is a useful diagnostic for multi-dimensional measurement of the plasma radiation. IRVB has been developed and installed in the Large Helical Device (LHD) [1-3]. Recently, IRVBs have been installed in KSTAR [4] and Alcator C-mod [5]. The preliminary design of the IRVB for JT-60SA has done [6].

In order to study the radiation phenomena toward reactor plasmas, i.e. ITER, the IRVB should be applied to the measurement in the neutron environment. Deuterium plasma experiment has started in LHD [7]. In order to apply the IRVB measurement to the neutron environment, a neutron shielding of an IR camera was required. Since the main focus of the IRVB measurement is plasma detachment, we can consider that the neutron emission rate is 3.3 × 10^{15} n·s^{-1}, which is predicted in the averaged discharge on LHD. In this paper, the design of the shielding for the IR camera using MCNP6 code is described and the operation result of the IR camera is reported.

II. Schematic of IRVB

The schematic of the IRVB for the LHD deuterium experiment is shown in Fig. 1. IRVB mainly consists of the pinhole camera section and the IR camera section. Plasma

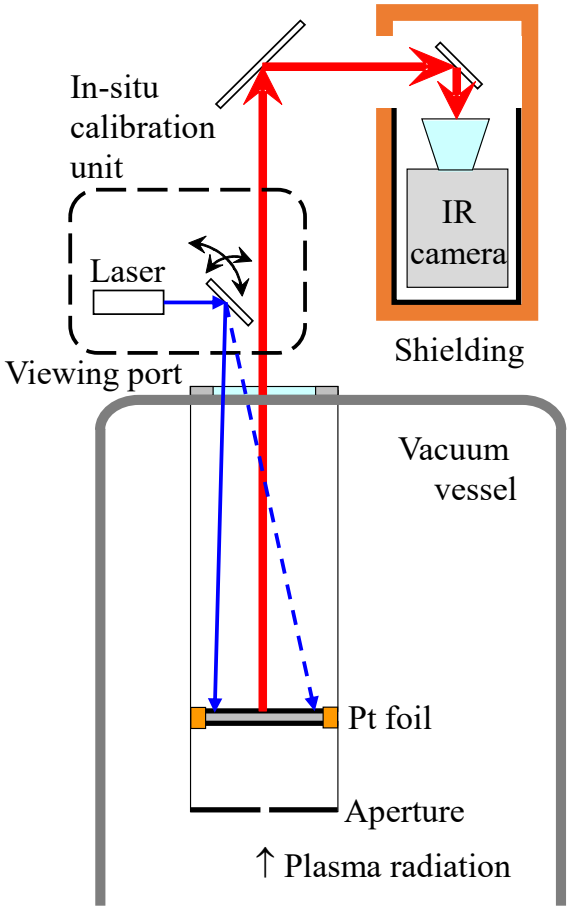

Fig. 1. Schematic of the InfraRed imaging Video Bolometer (IRVB) for the LHD deuterium experiment. Red-thick and blue-thin arrows indicate the path of the infrared signal and the He-Ne laser for in-situ calibration.

Manuscript received December XX, 2017; revised MM, DD, 2018. This work was supported by JSPS KAKENHI Grant Number JP17K14900 and by NIFS/NINS Grant Number NIFS16ULHH026.

K. Mukai is with National Institute for Fusion Science (NIFS), National Institutes of Natural Sciences and SOKENDAI (The Graduate University for Advanced Studies), 322-6 Oroshi-cho, Toki-shi, Gifu, 509-5292 Japan (e-mail: mukai.kiyofumi@nifs.ac.jp).

T. Nishitani is with NIFS.

K. Ogawa and B.J. Peterson are with NIFS and SOKENDAI.

radiation is projected onto the platinum foil detector through the aperture. The size of the foil detector is 130 mm × 100 mm × 2.5 μm. The foil detector is coated by carbon on both sides to increase the sensitivity. The temperature profile of the foil detector is observed from the backside using the IR camera (FLIR/ SC655). The IR camera is shielded from neutrons, gamma ray, and magnetic field. The in-situ calibration unit consists of a He-Ne laser and mirrors with motorized stages. In order to calibrate the thermal characteristics of the detector, the laser irradiation point can be scanned. The unit is removable to reduce the amount of the radiated material [8].

III. Guideline of Neutron Flux for Shielding Design

An IRVB had been installed in JT-60U tokamak [9]. An IR camera (FLIR (Indigo) / Omega) was used for the IRVB and it could be operated in the neutron emission rate up to 4 × 10^{15} n·s^{-1}. The model number of the IR camera is different from the IR camera for LHD, however, the detector type of the microbolometer is the same. Then, the operable neutron emission rate in JT-60U can be considered as a guideline for the design of the shielding in LHD. The major radius R of the JT-60U was 3.4 m and the IR camera was installed at around the minor radius r ~ 2.0 m with a shielding. The shielding consisted of polyethylene, lead, and soft iron with the thicknesses of 90 mm, 15 mm, and 20 mm, respectively. With the assumptions that (i) neutrons diffuse isotropically from the simple torus with the R = 3.4 m, that (ii) the neutrons are not shielded by the vacuum vessel, and that (iii) the neutron flux decreases 90% due to the polyethylene, the neutron flux in the shielding can be estimated as 1 × 10^{8} n·cm^{-2}·s^{-1}.

In order to investigate the irradiation effect on the IR camera which is used in JT-60U (FLIR (Indigo) / Omega), the irradiation test was performed in OKTAVIAN [10]. After the irradiation with a neutron flux of 7 × 10^{5} n·cm^{-2}·s^{-1} for three hours, a small number of dead pixels were observed [11]. The effect was transient since the dead pixels disappeared after the reboot of the IR camera. Here, the total neutron fluence was 8 × 10^{9} n·cm^{-2}. When the discharge duration in JT-60U is considered to be approximately 10 s, the neutron flux of 1 × 10^{8} n·cm^{-2}·s^{-1} discussed above is appropriate for the guideline for the design.

The maximum neutron emission rate of the LHD deuterium experiment is predicted to be 1.9 × 10^{16} n·s^{-1} [12]. Here, the main target of the IRVB measurement is plasma detachment. For such discharges, we can consider the neutron emission rate of 3.3 × 10^{15} n·s^{-1} which is predicted in the averaged discharge on LHD. In the calculation using the MCNP Monte Carlo neutronics code (MCNP6) [13], the result output is the neutron flux per one neutron. Then, to reduce the neutron flux below 1 × 10^{8} n·cm^{-2}·s^{-1} in the shielding, the output should be less than 3 × 10^{-8} cm^{-2}·s^{-1} for the averaged discharge.

IV. Concept Design and Neutron Flux Estimation

MCNP6 code with the three-dimensional modeling of LHD [14] and with the cross-section library of ENDF B-VI [15] was used to estimate the neutron flux and to design the shielding of the IR camera. The concept design is as follows. (i) Since the IR camera is installed close to the upper port of LHD (6.5-U), the neutron flux from the bottom side of the shielding can be considered as stronger than the flux from other sides. Then, the thickness of the polyethylene on the bottom side should be larger than the thickness on the other side. (ii) According to the previous estimation, not only the 2.45 MeV neutrons from D-D reaction but also the scattered neutrons were observed in the torus hall [14]. Hence the influence of the neutron flux from a lens hole should be reduced. (iii) The size of the shielding should be small and the weight of the shielding should be light as possible.

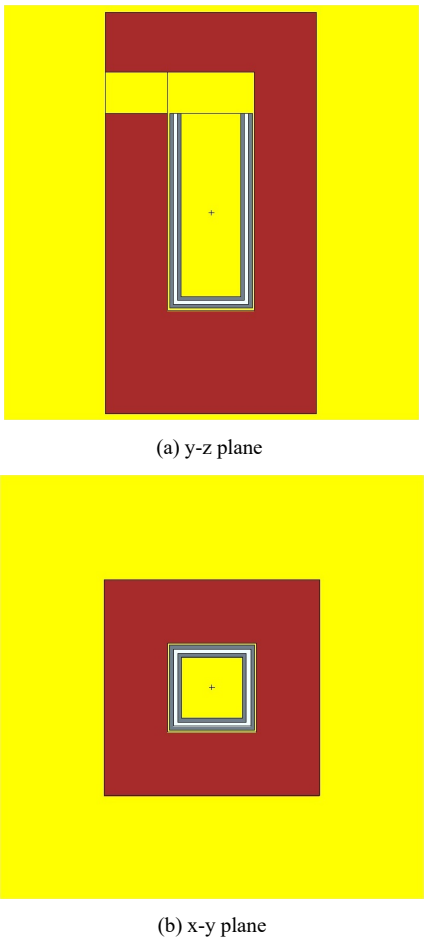

(a) y-z plane

(b) x-y plane

Fig. 2. Model of the shielding for the IR camera. Yellow hatch indicates air. Brown, gray, and white hatches indicate polyethylene, soft iron, and tungsten sheet, respectively. The IR camera is installed around the center of the shielding.

The shielding was designed as shown in Fig. 2. The size of the shielding is 510 mm × 510 mm × 970 mm. The lens hole is located on the left side in Fig. 2 (a) with the size of 100 mm × 100 mm. Polyethylene colored by brown in Fig. 2 is used for the neutron shielding with the thickness of 250 mm on the bottom side and 150 mm on the other sides. Soft iron colored by gray in Fig. 2 is used for the magnetic field shielding. The magnetic shielding which was used before the LHD deuterium experiment has been doubled and the thickness is 9 mm for each. The gap of the double magnetic shield is filled with the high density tungsten sheet (Nippon Tungsten) [16] of 9 mm thickness. The tungsten sheet consists of tungsten powder and resin. It has equivalent neutron shielding effect to lead without the risk of lead pollution. The IR camera is installed upward and observes the temperature profile on the foil detector using the two mirrors as shown in Fig. 1.

The neutron flux calculated by using MCNP6 code is shown in Fig. 3. The red color indicates the neutron flux per neutron over 3 × 10^{-8} cm^{-2}·s^{-1} which corresponds to the guideline for the averaged discharge. The strong neutron flux

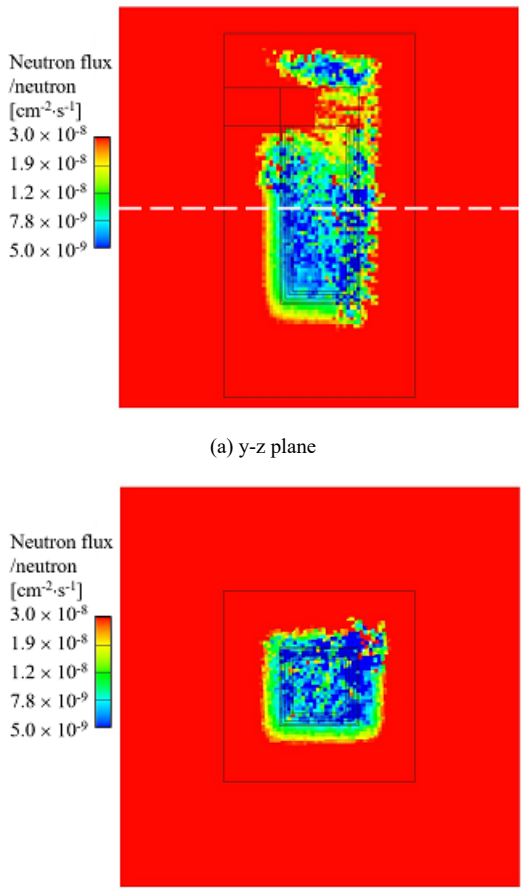

(a) y-z plane

(b) x-y plane

Fig. 3. Profiles of neutron flux per neutron calculated using MCNP6 code. Red color indicates that the IR camera is difficult to operate with the averaged discharge condition in LHD.

from the lens hole could be avoided using the mirror inside the shielding as shown in Fig. 3 (a). Fig. 3 (b) shows the neutron flux profile in the cross-section which corresponds to the position of the IR camera detector approximately and described as the dashed line in Fig. 3 (a). The neutron flux per neutron in the shielding was calculated 8.9×10^{-9} $cm^{-2}\cdot s^{-1}$ which is lower than the guideline of 1×10^{-8} $cm^{-2}\cdot s^{-1}$. This result indicates that the IR camera can be operated with the neutron emission rate up to 1×10^{16} $n\cdot s^{-1}$, which is sufficiently higher than the targeted condition of the IRVB measurement.

V. IR Camera Operation with Shielding in LHD Deuterium Experiment

The designed shielding was installed as shown in Fig. 4 and applied to the LHD deuterium experiment. The IR camera requires an Ethernet cable and two coaxial cables for supplying power and for triggering. The cable hole for these cables has small labyrinth structure. The in-situ calibration unit can be installed in the hatched space.

The deuterium plasma experiment was started from March 7, 2017. In the first experimental campaign, the maximum neutron emission rate of 3.3×10^{15} $n\cdot s^{-1}$ [17] and the total neutron emission of 3.6×10^{18} n was measured. The MCNP6 calculation in section IV estimates the maximum neutron emission rate of 2.9×10^{7} $n\cdot s^{-1}$ and the total neutron emission of 3.2×10^{10} n at around the IR camera. The IR camera image at the end of the discharge is shown in Fig. 5. The frame rate

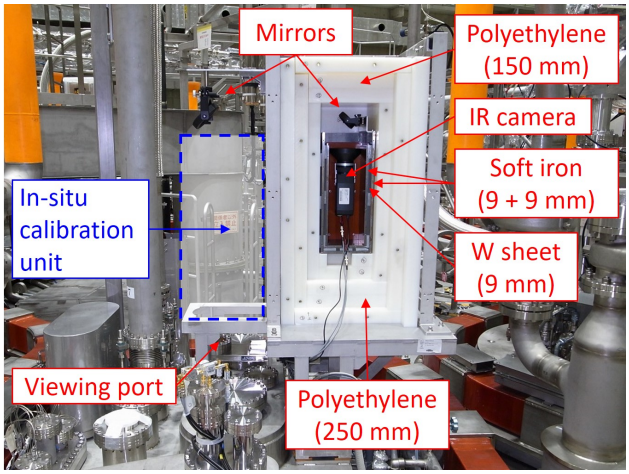

Fig. 4. Schematic of the shielding for the IR camera installed in LHD.

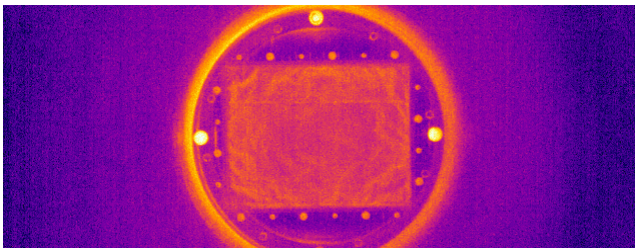

Fig. 5. IR camera image at the end of the discharge which obtained the maximum neutron emission rate of 3.3×10^{15} $n\cdot s^{-1}$ (#140932). No dead pixels were observed. The rectangular part at the center is the foil detector as shown in Fig. 1.

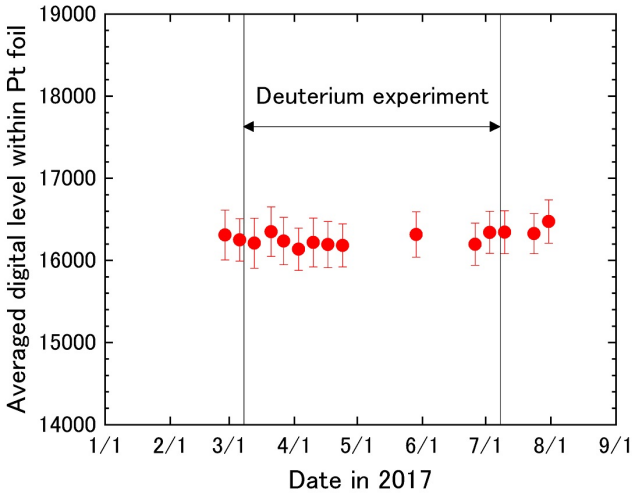

Fig. 6. Variation of IR camera digital level averaged over all pixels for Pt foil. Foil temperature was almost constant due to the baking of the LHD first wall.

was 100 Hz and the camera pixel number was 640 × 240. Because the shielding works as designed, no dead pixels were observed. Fig. 6 indicates the variation of the IR camera digital level before and after the deuterium experiment. The foil temperature was almost fixed due to the baking of the LHD first wall. The error bar was determined as the range of the maximum and minimum values. Obviously difference of the digital level was not observed after the neutron irradiation.

VI. Summary And Future Work

For the application of the IRVB measurement to the LHD deuterium experiment, the neutron shielding for the IR camera was designed. The main purpose of the measurement is to

investigate the plasma radiation phenomena such as detachment. In this case, the neutron emission rate can be considered as 3.3×10^{15} $n \cdot s^{-1}$ which is predicted in the averaged discharge on LHD. The shielding was designed using MCNP6 code with the three-dimensional modeling of LHD based on the operational experience in the JT-60U and the result of the irradiation test in OKTAVIAN. The polyethylene thickness on the bottom side was thickened with consideration for the neutron flux from the installation port. The neutron flux through the lens hole was avoided using two mirrors. The designed shielding was installed and applied to the LHD deuterium experiment. The IRVB could be operated successfully without any dead pixel in the emission rate up to 3.3×10^{15} $n \cdot s^{-1}$ and in the total neutron emission of 3.6×10^{18} n. These correspond to the neutron emission rate of 2.9×10^{7} $n \cdot s^{-1}$ and the total neutron emission of 3.2×10^{10} n at around the IR camera. IR cameras are used in fusion plasma devices, e.g., for the divertor thermography and the thermal monitor. The shielding design discussed in this paper can be applied to these diagnostics. Moreover, since IR cameras are too costly for neutron irradiation test, the further experience which will be obtained in the LHD deuterium experiment can provide useful information also to the other fusion devices.

The IRVB also uses the foil detector as a primary detector. In order to investigate the neutron irradiation effect on the thermal characteristics, (1) development of the laser irradiation system and (2) improvement of the reproducibility and uniformity of the carbon coating on the foil detector are required. The IRVB measurement can be applied basically to the neutron environment after these improvements.

ACKNOWLEDGMENT

The first author would like to thank NIFS technical staff for their support of the irradiation test in OKTAVIAN and of the IRVB installation and operation.

REFERENCES

[1] B.J. Peterson, M. Osakabe, M. Shoji, and N. Ashikawa, “Infrared imaging video bolometer for the large helical device,” Rev. Sci. Instrum., vol 72, pp. 923-926, 2001.

[2] K. Mukai, B.J. Peterson, S.N. Pandya, R. Sano, and M. Itomi, “Improvement of Infrared Imaging Video Bolometer Systems in LHD,” Plasma Fusion Res., vol. 9, pp. 3402037-1 - 3402037-5, 2014.

[3] K. Mukai et al., “Development of impurity seeding and radiation enhancement in the helical divertor of LHD,” Nucl. Fusion, vol. 55, pp. 083016 (9pp), 2015.

[4] J.H. Jang et al., “Two-dimensional Radiation Profiles Using an Infrared Imaging Video Bolometer (IRVB) During Krypton Seeding in KSTAR,” presented at the 22nd Topical Conference on High Temperature Plasma Diagnostics, San Diego, USA, Apr. 16-19, 2018.

[5] M.L. Reinke et al., “Experimental Tests of an Infrared Video Bolometer on Alcator C-Mod,” presented at the 22nd Topical Conference on High Temperature Plasma Diagnostics, San Diego, USA, Apr. 16-19, 2018.

[6] R. Sano, K. Mukai, B.J. Peterson, M. Fukumoto, and K. Hoshino, “Conceptual design of imaging bolometer for use of computed tomography in JT-60SA”, Rev. Sci. Instrum., vol 88, pp. 053506-1 – 053506-10, 2017.

[7] T. Morisaki et al., “Overview of Initial Results of LHD Deuterium Experiment,” The 21st International Stellarator-Heliotron Workshop, I-1, Kyoto, 2017.

[8] K. Mukai, B.J. Peterson, S. Takayama, and R. Sano, “In situ calibration of the foil detector for an infrared imaging video bolometer using a carbon evaporation technique,” Rev. Sci. Instrum., vol 87, pp. 11E124-1 - 11E124-3, 2016.

[9] S. Konoshima, B.J. Peterson, N. Ashikawa, Y. Miura, and the JT-60 team, “Radiated Power Profile Observed by a Tangentially Viewing IR Imaging Bolometer in JT-60U Tokamak,” 32nd EPS Conference on Plasma Phys., ECA Vol. 29C, P-4.092, 2005.

[10] I. Murata et al., “Compendium of Neutron Beam Facilities for High Precision Nuclear Data Measurements,” IAEA-TECDOC-1743 (Vienna: IAEA), pp 110–18, 2014.

[11] K. Ogawa et al., “Investigation of irradiation effects on highly integrated leading-edge electronic components of diagnostics and control systems for LHD deuterium operation,” Nucl. Fusion, vol. 57, pp. 086012 (7pp), 2017.

[12] M. Osakabe et al., “Current Status of Large Helical Device and Its Prospect for Deuterium Experiment,” Fusion Sci. Technol., vol. 72, pp. 199-210 2017.

[13] X-5 Monte Carlo Team, “MCNP User’s Guide - Code Version 6.1.1beta,” LA-CP-14-00745 Los Alamos National Laboratory, Los Alamos, 2014.

[14] T. Nishitani, K. Ogawa, K. Nishimura, and M. Isobe, “Radiation Field Estimation for the Diagnostic and Control Components by Monte Carlo Neutronics Calculations with LHD 3-Dimensional Modeling,” Plasma Fusion Res., vol. 11, pp. 2405057-1 - 2405057-4, 2016.

[15] H.D. Lemmel, et al., “ENDF/B-VI Release 8 (Last release of ENDF/B-VI),” The U.S. Evaluated Nuclear Data Library for Neutron Reaction Data, IAEA-NDS-100, Rev. 11, IAEA, Vienna, 2001.

[16] NIPPON TUNGSTEN CO.,LTD., HIGH DENSITY TUNGSTEN SHEET, https://www.nittan.co.jp/en/products/tungsten_sheet_008_033.html (accessed Apr. 27, 2018)

[17] K. Ogawa et al., “Enhancement of energetic-particle physics studies by using a comprehensive neutron diagnostics in helical plasmas,” The 21st International Stellarator-Heliotron Workshop, P1-25, Kyoto, 2017.